Journal of Virology®

PATHOGENESIS AND IMMUNITY

A Morbillivirus Infection Shifts DC Maturation Toward a Tolerogenic Phenotype to Suppress T Cell Activation

Daniel Rodríguez-Martín,[a] Isabel García-García,[b] Verónica Martín,[a] José Manuel Rojas,[a] Noemí Sevilla[a]

[a]Centro de Investigación en Sanidad Animal (CISA-INIA-CSIC), Instituto Nacional de Investigación y Tecnología Agraria y Alimentaria, Consejo Superior de Investigaciones Científicas, Valdeolmos, Madrid, Spain

[b]Departamento de Genética, Fisiología y Microbiología, UD de Genética, Facultad de CC. Biológicas, Universidad Complutense de Madrid, Madrid, Spain

ABSTRACT Viruses have evolved numerous strategies to impair immunity so that they can replicate more efficiently. Among those, the immunosuppressive effects of morbillivirus infection can be particularly problematic, as they allow secondary infections to take hold in the host, worsening disease prognosis. In the present work, we hypothesized that the highly contagious morbillivirus peste des petits ruminants virus (PPRV) could target monocytes and dendritic cells (DC) to contribute to the immunosuppressive effects produced by the infection. Monocytes isolated from healthy sheep, a natural host of the disease, were able be infected by PPRV and this impaired the differentiation and phagocytic ability of immature monocyte-derived DC (MoDC). We also assessed PPRV capacity to infect differentiated MoDC. Ovine MoDC could be productively infected by PPRV, and this drastically reduced MoDC capacity to activate allogeneic T cell responses. Transcriptomic analysis of infected MoDC indicated that several tolerogenic DC signature genes were upregulated upon PPRV infection. Furthermore, PPRV-infected MoDC could impair the proliferative response of autologous $CD4^+$ and $CD8^+$ T cell to the mitogen concanavalin A (ConA), which indicated that DC targeting by the virus could promote immunosuppression. These results shed new light on the mechanisms employed by morbillivirus to suppress the host immune responses.

IMPORTANCE Morbilliviruses pose a threat to global health given their high infectivity. The morbillivirus peste des petits ruminants virus (PPRV) severely affects small-ruminant-productivity and leads to important economic losses in communities that rely on these animals for subsistence. PPRV produces in the infected host a period of severe immunosuppression that opportunistic pathogens exploit, which worsens the course of the infection. The mechanisms of PPRV immunosuppression are not fully understood. In the present work, we demonstrate that PPRV can infect professional antigen-presenting cells called dendritic cells (DC) and disrupt their capacity to elicit an immune response. PPRV infection promoted a DC activation profile that favored the induction of tolerance instead of the activation of an antiviral immune response. These results shed new light on the mechanisms employed by morbilliviruses to suppress the immune responses.

KEYWORDS PPRV, monocyte, tolerance, immunosuppression, monocyte-derived DC, sheep, monocyte-derived dendritic cell

Peste des petits ruminants (PPR) is an infection disease of wild and domestic small ruminants that primarily affects sheep and goats. It was first described in 1942 in Côte d'Ivoire (1), but its current distribution covers North, East, West and Central Africa, the Middle East, and Asia, regions where the disease is considered endemic (2). PPR is an acute disease, with animals usually dying 4 to 6 days after the onset of fever, with mortality rates up to 90% in naive populations; it also produces abortion of pregnant

Editor Stacey Schultz-Cherry, St. Jude Children's Research Hospital

Address correspondence to Noemí Sevilla, sevilla@inia.csic.es, or José Manuel Rojas, rojas.jose@inia.csic.es.

The authors declare no conflict of interest.

Received 11 August 2022
Accepted 18 August 2022
Published 12 September 2022

animals (3). PPR causes an estimated economic loss worth $1.2 to $1.7 billion per year, with dire economic and social consequences for entire communities that heavily depend on sheep and goats as their main livelihood. PPR has been marked as the next viral pathogen to be eradicated by 2030 by the World Organisation for Animal Health and FAO (4).

Peste des petits ruminants virus (PPRV) is the causative agent of PPR disease. PPRV has a linear nonsegmented negative-sense single-stranded RNA genome. It is a member of the *Paramyxoviridae* family, *Morbillivirus* genus, which includes other relevant pathogens such as measles virus (MV), rinderpest virus (RPV), and canine distemper virus (CDV) (5). The typical incubation period of the virus is 2 to 7 days, with signs that include fever, oculonasal discharge, diarrhea, leukopenia, dyspnea, and sloughing of the epithelium of the oral and nasal mucosae (3). Transmission occurs via aerosol droplets, and infection is thought to begin with PPRV taken up by antigen-presenting cells (APCs) within the respiratory mucosa. These infected APC then migrate to regional lymphoid tissues where the virus can start replication (3, 6, 7). PPRV shows a tropism for lymphoid and epithelial tissues, as the virus interacts with the host cells through two receptors, signaling lymphocyte activation molecule (SLAM/CD150) and nectin-4. SLAM/CD150 is the main cellular receptor of morbilliviruses, exclusively expressed on the surface of immune cells such as lymphocytes, macrophages, and dendritic cells (DC) (3, 7, 8), whereas nectin-4 is principally expressed on epithelial cells.

Owing to this lymphoid tropism, PPRV infections are characterized by an acute immunosuppression that favors the onset of secondary infections that complicate the clinical outcome of the disease. There is evidence that PPRV can profoundly affect the activation process of T cells since polyclonal T cell responses to the mitogen ConA are impaired for at least 15 days postinfection (9, 10). Since DC are central for initiating effective T cell responses, it could be hypothesized that PPRV could target these cells to mediate its immunosuppressive effects.

DC are a diverse group of leukocytes, key for the immune system as they play an important role as APC. Their role includes the induction and regulation of the adaptive immune response by acting as a bridge between innate and adaptive immunity (11, 12). Located in submucosal tissues, DC survey for incoming pathogens to capture and process the pathogen antigens. As a consequence of recognizing pathogen-associated molecular patterns (PAMP) (such as viral genetic material) through their pattern recognition receptors (PRR), DC become activated and subsequently migrate to secondary lymphoid organs so that they can trigger T cell responses. DC ability to recognize invading pathogens and become activated is therefore the first critical step in the development of an adequate immune response (11, 13). As a result of their central role in immunity, several viruses are known to target DC, including the morbilliviruses MV and CDV (14–18).

Since DC primarily exist in two basic functional states, immature (iDC) and mature (mDC) (19), we have studied the effects of PPRV infection in both cell phases in a natural host of the disease. Monocyte-derived dendritic cells (MoDC), a subset of functional DC that can be obtained *in vitro* from monocytes cultured with granulocyte-macrophage colony-stimulating factor (GM-CSF) and interleukin-4 (IL-4) (20), are the perfect tool to study PPRV infection effects on ovine DCs since they can be obtained in relatively large numbers. In the present work we determined whether PPRV affects the development of immature MoDC. We also performed transcriptomic and functional analyses of infected mature MoDC to assess the consequences of viral infection on the activity of mDC. We present evidence of the multifaceted effects triggered by morbillivirus infection on DC biology that could act as a mechanism that contributes to host immunosuppression.

RESULTS

PPRV productively infects CD14$^+$ cells without significantly increasing cell death. To determine PPRV effects on DC, we first established a differentiation protocol for ovine monocyte-derived DC (MoDC) using recombinant ovine Gm-CSF (OvGM-CS)F and ovine IL-4 (OvIL-4) (Fig. S2 in the supplemental material). MoDC thus upregulated

upon differentiation characteristic DC markers (CD11b, CD11c, CD209, CD80, CD86, major histocompatibility complex class I (MHC-I), major histocompatibility complex class II (MHC-II), CD1 and CD1w2) and could be matured by 24-h poly(I·C) stimulation. Immature MoDC (iMoDC) had high phagocytic capacity, while mature MoDC (mMoDC) could stimulate the proliferation of allogeneic T cells. Therefore, functional iMoDC and mMoDC could be obtained using this protocol.

We next evaluated PPRV capacity to infect $CD14^+$ cells and, as a consequence, affect their differentiation to iMoDC. Freshly isolated $CD14^+$ were infected with PPRV-ICV'89 at a multiplicity of infection (MOI) of 1 and subsequently differentiated into iMoDCs with OvGM-CSF and OvIL-4. PPRV infection was monitored by flow cytometry using anti-PPRV-N protein intracellular staining. Seventy-two hours postinfection approximately 40% of cells were positive for the PPRV-N protein (Fig. 1A). Plaque assays of culture supernatants at different time points postinfection (Fig. 1B) showed an increase in virus titer with time, indicating that PPRV is capable of productively infecting monocytes while they differentiate into iMoDC. In many cases, viral infections enhance DC apoptosis, thus weakening a major body defense line (21). Annexin V and 7-AAD staining was performed on mock- and PPRV-infected cells at 24, 48, and 72 h postinfection (hpi) to determine whether PPRV-induced apoptosis on differentiating iMoDC (Fig. 1C and D). Our data showed that the percentage of late apoptotic cells increased at late infection points (72 hpi) when compared to early time points (24 hpi) both in mock- and PPRV-infected iMoDC (Fig. 1D). The percentage of early (annexin V^+/7-AAD^-) or late (Annexin V^+/7-AAD^+) apoptotic cells in PPRV-infected iMoDC cultures was not significantly different from that in mock-infected counterparts. This indicates that PPRV does not significantly increase cell death in monocytes that differentiate to iMoDC.

PPRV infection of $CD14^+$ cells impairs the upregulation of critical surface DC molecules and the phagocytic function of iMoDC. To determine whether PPRV infection of $CD14^+$ cells disrupts differentiation to iMoDC, flow cytometry was used to assess the surface expression of phenotypic markers at 72 h after PPRV infection (Fig. 2A). PPRV-infected cells showed a statistically significant impaired upregulation in the characteristic DC adhesion molecule CD11c compared to mock cultures. Molecules associated with PAMP recognition were also reduced in PPRV-infected cells: expression of Toll-like receptor 4 (TLR4)-associated CD14 and the C-type lectin receptor CD209 was significantly lower in infected cells. Likewise, expression of antigen-presenting molecules MHC-II, CD1, and CD1w2 was also significantly lower on PPRV-infected cells than on control. Expression of costimulatory markers CD80 and CD86, adhesion molecules CD11b, and antigen-presenting MHC-I molecules showed no statistical differences between PPRV- and mock-infected cells. These data suggest that PPRV infection could affect iMoDC differentiation and impair cellular mechanisms involved in antigen processing, PAMP recognition and interaction with the milieu.

To study whether antigen uptake, one of the main functions of iMoDC, was affected by PPRV infection, we carried out microsphere phagocytosis assays comparing mock- and PPRV-infected iMoDC. Flow cytometry analysis (Fig. 2B and C) showed a statistically significant decrease in the total amount of internalized microspheres (reduced mean fluorescence instensity [MFI]) in infected iMoDC. To confirm that these microspheres were internalized by iMoDC, confocal microscopy studies were performed (Fig. 2D). Z-stack confocal images of PPRV- or mock-infected iMoDC revealed microsphere internalization. As shown in the orthogonal projections, confocal imaging also confirmed that PPRV-infected iMoDC internalized fewer microspheres than their mock-infected counterparts. These data indicate that PPRV infection reduces the phagocytic capacity of iMoDC.

PPRV replicates in MoDC. Due to DC relevance in activating immune responses, we addressed whether PPRV could infect MoDC as efficiently as monocytes. To this end, iMoDC differentiated for 48 h were infected with PPRV-ICV'89 at an MOI of 1. At 24 hpi, mock- and PPRV-infected iMoDC were matured with poly (I·C) stimulation overnight. At 48 hpi, mMoDC staining with anti-PPRV-N protein showed a high percentage of MoDC positive for PPRV-N (67% $\pm$ 7.5%) by flow cytometry (Fig. 3A). Furthermore,

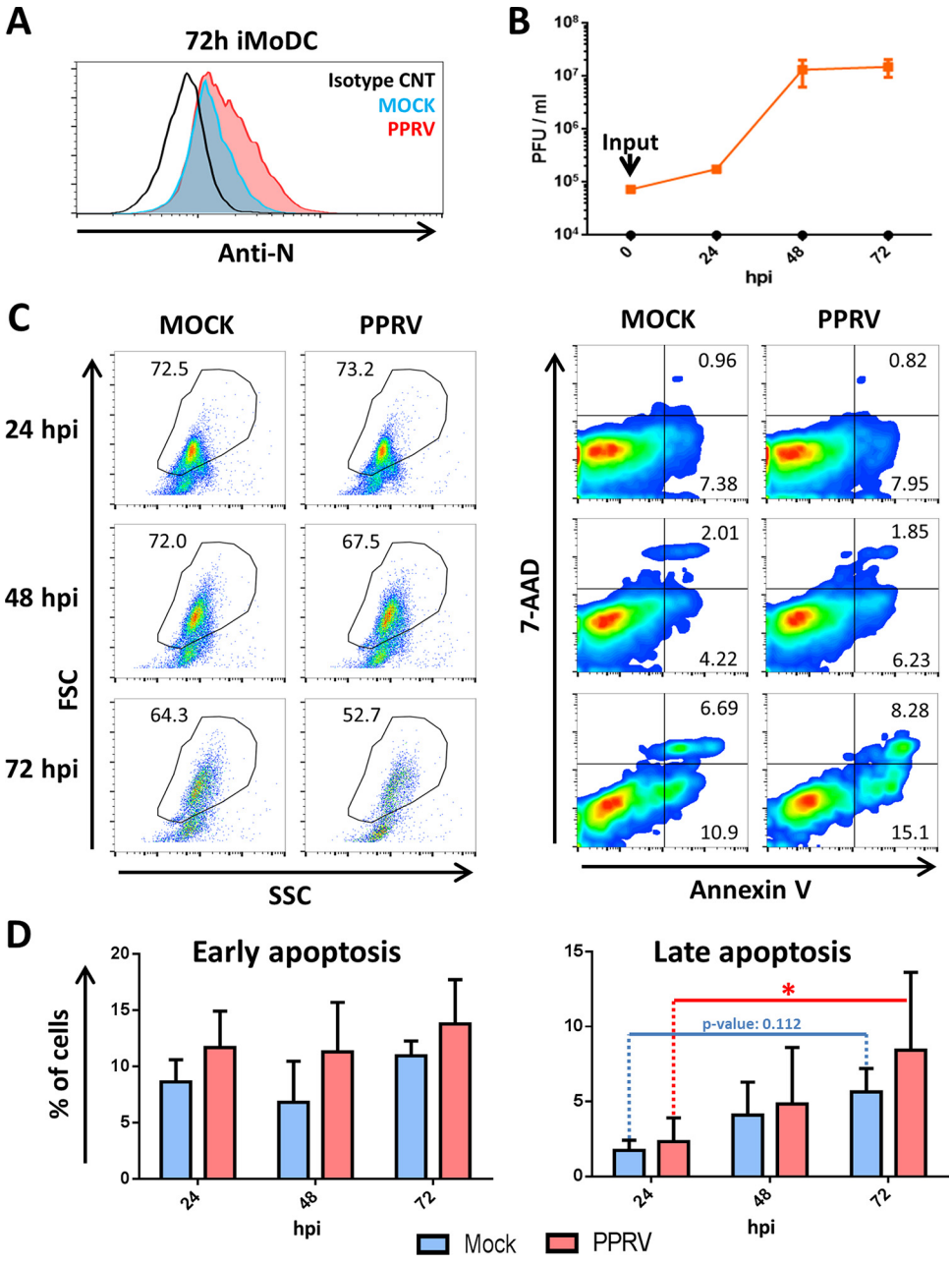

FIG 1 CD14$^+$ cell infection with PPRV and differentiation to iMoDC. Freshly isolated CD14$^+$ cells were infected with PPRV at an MOI of 1 (or mock-infected as control) and differentiated into iMoDC for 72 h. (A) Representative flow cytometry intracellular staining histogram using anti-PPRV-N monoclonal antibody in mock-infected (blue) and PPRV-infected (red) iMoDC. Isotype controls were included (black line). (B) Titration by plaque assays in VDS cell line of iMoDC culture supernatant at 0 (input), 24, 48, and 72 hpi. (C) Flow cytometry assessment of iMoDC death induced by PPRV infection at 24, 48, and 72 hpi. (Left) Representative iMoDC forward scatter/side scatter (FSC/SSC) dot plot and gating for Annexin V and 7-AAD staining analysis. (Right) Representative dot plots for Annexin V and 7-AAD staining in mock- or PPRV-infected cells. Numbers in lower right quadrant (Annexin V$^+$ 7-AAD$^-$) and in upper right quadrant (AnnexinV$^+$ 7-AAD$^+$) indicate, respectively, the percentage of early apoptotic and late apoptotic cells present in the culture. (D) Percentage of CD14$^+$ cells differentiating into iMoDC in early apoptosis state (left) and late apoptosis state (right) in PPRV$^+$ cultures (red), compared to that in mock-infected (blue) cells, at 24, 48, and 72 hpi ($n = 3$). *, $P < 0.05$; two-way analysis of variance (ANOVA) with Tukey's post-test.

the presence of infective virus in the supernatant of MoDC cultures indicated that the virus could productively replicate in MoDC (Fig. 3B).

Transcriptomic analysis of PPRV-infected ovine MoDC reveals a complex modulation of gene expression. Since PPRV can effectively infect DC, it has the potential to affect the biology of these cells. To obtain a global perspective of cellular changes induced by

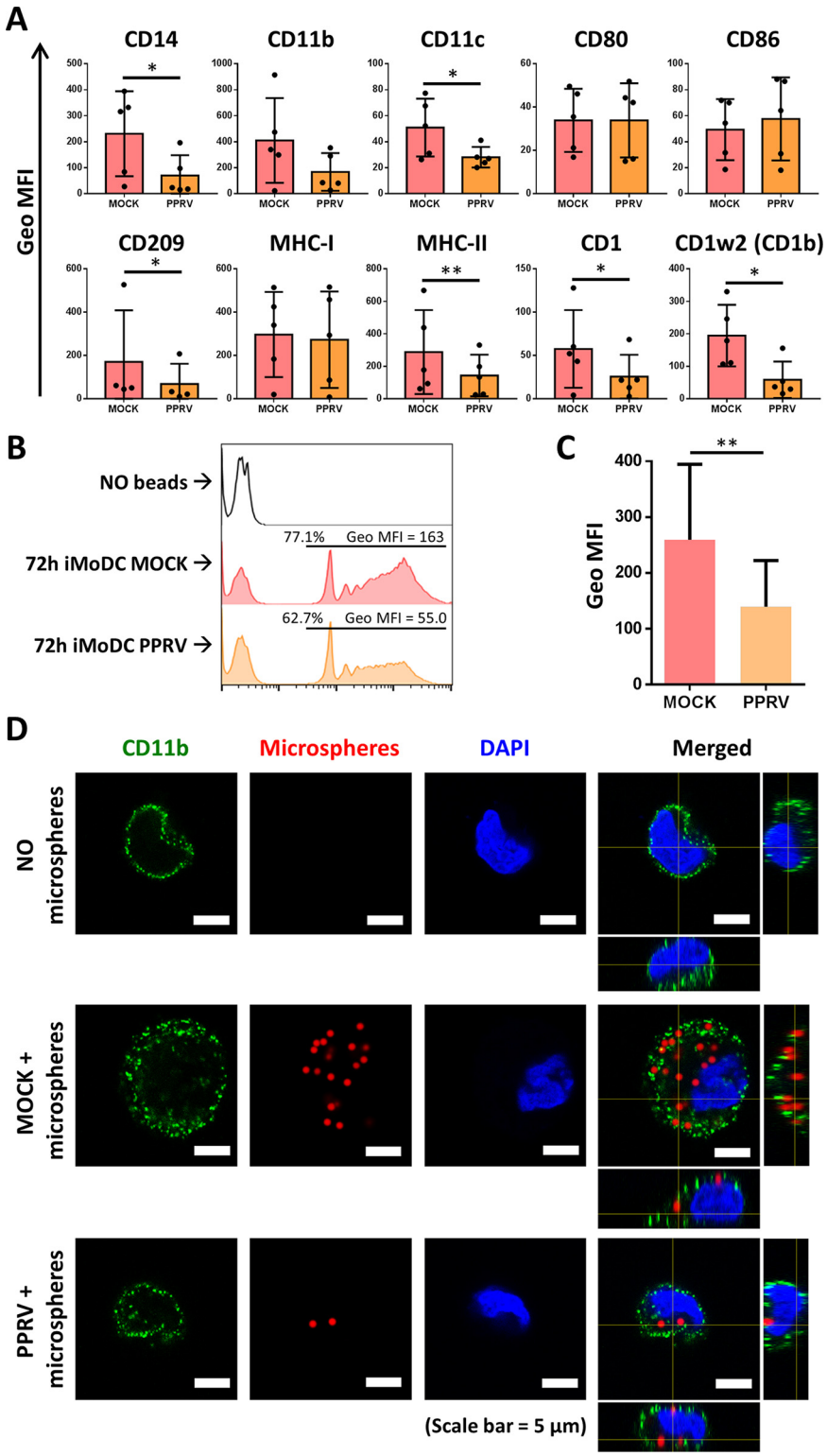

FIG 2 PPRV infection impairs iMoDC function. (A) Geometric mean fluorescence intensity (Geo MFI) of cell surface markers (mean ± SD) measured by flow cytometry in mock-infected (red) and PPRV-infected (orange) iMoDC measured in 4 or 5 donor sheep. *, $P < 0.05$; **, $P < 0.01$; multiple-ratio paired *t* test with Bonferroni-Dunn correction. (B) Microsphere phagocytosis assay assessed by flow cytometry, showing a decrease in both the percentage of cells and the number of beads (Geo MFI) captured by PPRV-infected iMoDC (orange) compared to mock-infected iMoDC (red). As a control, the histogram for iMoDC cultured without microspheres is shown (black line). (C) Geo MFI (mean ± SD) ($n = 3$) of PPRV-infected (red) and mock-infected (orange) iMoDC in microsphere phagocytosis assay assessed by flow cytometry. **, $P < 0.01$;

(Continued on next page)

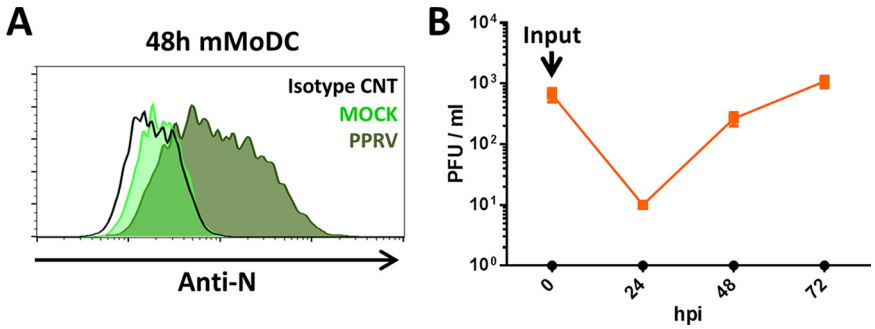

FIG 3 PPRV can productively infect MoDC. (A) Representative flow cytometry intracellular staining using anti-PPRV-N monoclonal antibody in mock-infected (bright green) and PPRV-infected (dark green) mMoDC. Isotype controls were included (black line). (B) Titration by plaque assay in VDS cell line of mock- or PPRV-infected MoDC culture supernatants at 0 (input), 24, 48, and 72 hpi. CNT, control.

PPRV on MoDC, we conducted RNA-sequencing (RNA-seq)-based transcriptomic analyses to characterize differential gene expression between PPRV- and mock-infected MoDC. The principal-component analyses (PCoA) on all samples arranged them in two groups: one contained the mock samples, while in the other, the PPRV samples were clustered (Fig. 4A). The analysis also revealed 688 differentially expressed genes (DEG) between PPRV- and mock-infected samples. Of these, 518 genes were upregulated while 170 genes were downregulated (Fig. 4B). We also assessed for the presence of PPRV mRNA in the samples (Table 1). Transcripts for all PPRV genes were detected in PPRV-infected MoDC, while none were detected in mock-infected samples. This confirms the PPRV infection of MoDC shown in Fig. 3. Transcript quantification also revealed that mRNA counts for each PPRV gene coincided with the characteristic "start-stop" transcription mechanism of paramyxoviruses (3). Interestingly, we also detected, for the first time to the best of our knowledge, the presence of transcripts for the PPRV-W gene during the infection. Since V and W transcripts are produced by the insertion of 1 or 2 guanine residues, respectively, at the conserved RNA editing site of the P gene (3), sequenced transcripts with these insertions were counted. C transcripts could not be quantified, as the C protein expression results from the leaky scanning of the P mRNA (3).

To determine the MoDC signaling and biological functions that were affected by the infection, sequencing data analysis based on gene set enrichment analysis (GSEA) and over-representation analysis (ORA) with the Kyoto Encyclopedia of Gene and Genome (KEGG) database (ORA-KEGG) were carried out. Overall, these analyses concurred in the signaling pathways that were modulated by the infection (Fig. 5). GSEA and functional ORA-KEGG detected statistically significant enrichment in signaling pathways related to autophagy regulation, viral recognition, cytokine signaling, and cell survival and activation. Upregulation of genes in the AMPK, mTOR, and phosphatidylinositol 3-kinase (PI3K)-Akt signaling pathways, which are related, among other things, to autophagy regulation, were detected in both analyses. Genes related to signaling pathways involved in viral infection sensing (NOD-like receptor, Toll-like receptor, and NF-κB signaling pathways) were also enriched according to GSEA and ORA-KEGG. Genes from the proinflammatory tumor necrosis factor (TNF) signaling pathway were found to be upregulated by both analyses. Concomitantly, genes from the immune regulatory tumor growth factor β (TGF-β) signaling pathways were also enriched in PPRV-infected MoDC using both analyses. GSEA also revealed the downregulation of over 50 genes related to the interferon (IFN) response (Fig. 5B). This indicates that a complex cytokine response takes place in the MoDC as a result of the infection, which involves proinflammatory as well as immune regulatory signals. Genes related to the mitogen-activated protein kinase (MAPK) and p53 pathways, which are important for cell activa-

FIG 2 Legend (Continued)
paired Student's *t* test. (D) Confocal images of microsphere phagocytosis assays in mock- or PPRV-infected iMoDC. iMoDC were stained for the membrane marker CD11b (green) and counterstained with DAPI (blue) to visualize nucleic acids. Crimson carboxylate-modified fluorescent microspheres are shown in red. Merged orthogonal projections were generated using ImageJ software. Scale bar = 5 μm.

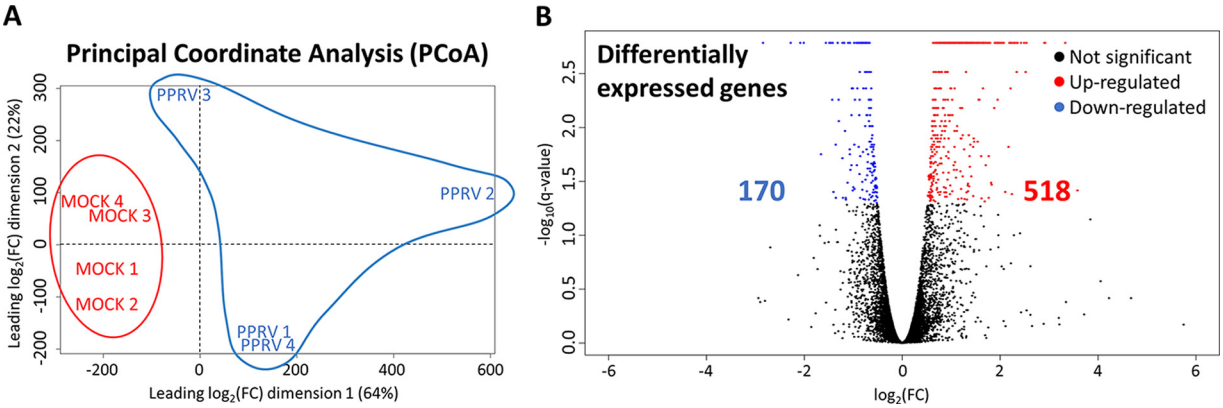

FIG 4 General results of RNA-seq data. (A) Two-dimensional scatterplot of the principal-coordinate analysis (PCoA) results showing the first two leading dimensions. Data clustered in two groups: PPRV-infected samples (blue) and mock-infected samples (red). (B) Volcano plot of gene expression values of PPRV-infected mMoDC compared to mock-infected controls, displayed as $\log_2$ fold change (FC) against statistical significance ($-\log_{10}$ [*q* value]). Red dots indicate significantly upregulated genes, blue dots indicate significantly downregulated genes, and black dots show genes with no significant differences.

tion and survival, were also modulated during the infection. Overall, it appears that MoDC are capable of recognizing the viral infection, as indicated by the enrichment of viral recognition signaling pathways. This probably triggers a complex cellular response in which autophagy, cell activation, and survival, as well as cytokine responses, are involved.

GSEA and transcriptomic ORA-KEGG was also applied to biological functions related to immune processes (Fig. 6). ORA-KEGG confirmed that genes related to biological functions associated with autophagy (phagosome, lysosome, and animal autophagy) were upregulated (Fig. 6A). The biological function "lysosome" was also enriched according to the GSEA (Fig. 6B). GSEA and ORA-KEGG also detected the biological process of "apoptosis" as significantly modulated in PPRV-infected MoDC with up- and downregulation of several genes. The analyses also concurred on the enrichment of the biological functions related to viral infection. Interestingly, ORA-KEGG found that 10 genes associated with the response to the prototypical morbillivirus MV were upregulated in PPRV-infected mMoDC (Fig. 6A), indicating that PPRV and MV infection share some characteristics. GSEA also identified the biological functions of DC and inflammatory response as upregulated, while antigen presentation was downregulated. Overall, biological function analysis confirmed the activation of autophagy and the modulation of apoptosis by PPRV. Moreover, both GSEA and ORA-KEGG identified that viral infection biological processes are modulated because of the infection. From an immunological perspective, the transcriptomic analysis showed that MoDC response to PPRV infection is complex. On the one hand, viral infection is recognized, which probably leads to the activation of an inflammatory response, while on the other hand, antigen presentation is reduced and the immunoregulatory TGF-β signaling

TABLE 1 Number of counts per million mapped reads for PPRV gene products detected in PPRV-infected mMoDC at 48 hpi

	PPRV-infected mMoDCs samples				
PPRV gene product	PPRV 1	PPRV 2	PPRV 3	PPRV 4	Avg
N	315,840	296,837	316,257	307,978	309,228
P[a]	306,468	296,621	293,291	279,353	293,933
M	13,7499	137,064	139,936	141,015	138,879
H	93,692	92,956	95,692	94,937	94,319
F	85,952	83,849	83,847	82,952	84,150
L	43,376	40,494	43,060	45,190	43,030
V[a]	32,706	33,540	31,910	32,450	32,652
W[a]	21	44	33	51	37

[a]V and W transcripts result from an RNA editing site present in the P gene that leads to the insertion of 1 G residue for V or 2 G residues for W (3). Only unique sequence matches were mapped to transcript species; thus only unequivocal counts for P, V and W are shown. C transcripts cannot be identified as the C protein translation results from the leaky scanning of the P transcripts (3).

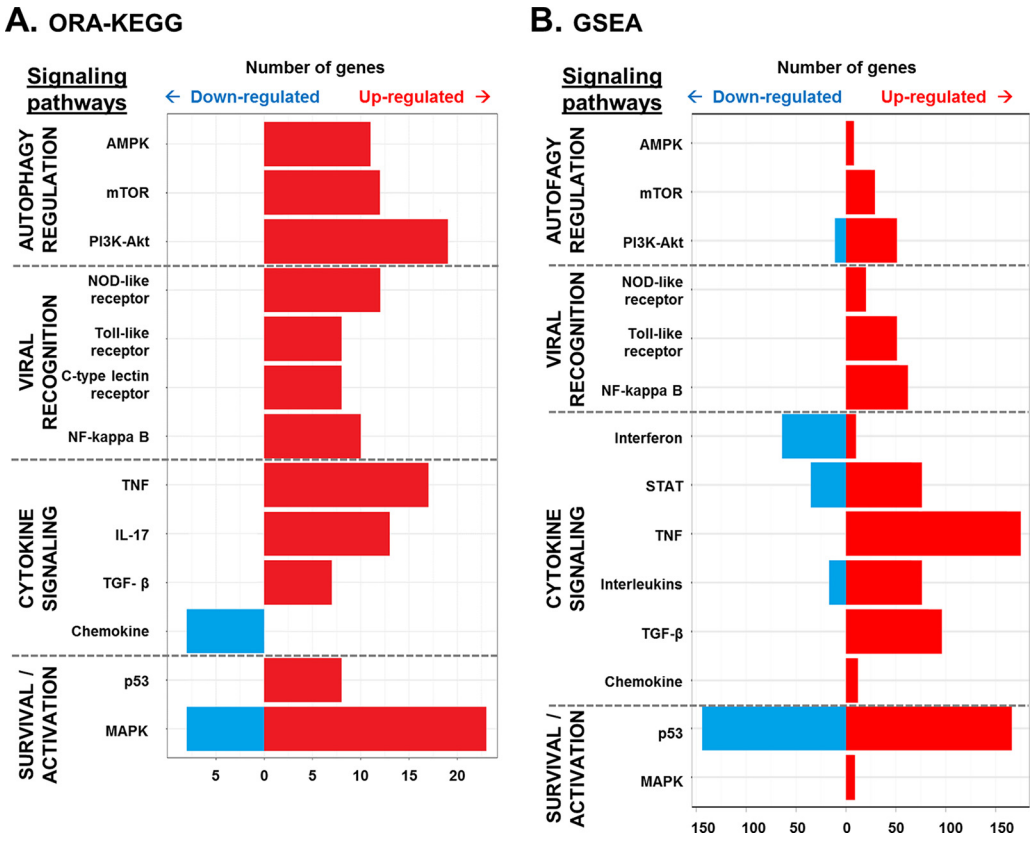

FIG 5 Multiple signaling pathways are affected by PPRV infection in mMoDC. Shown are the numbers of genes involved in statistically significant upregulated (red) and downregulated (blue) signaling pathways related to autophagy regulation, viral recognition, cytokine signaling, and cell survival and activation obtained by ORA-KEGG (A) or GSEA (B) analysis in PPRV-infected mMoDC compared to mock-infected mMoDC.

pathway is triggered upon infection. The balance between these processes will dictate PPRV effect on MoDC activity.

PPRV impairs ovine MoDC antigen-presenting capacity. To further our understanding of the infection effects on DC, we carried out experiments to study the functionality of PPRV-infected MoDC. Mature DC are the only cells able to activate naive T cells, and this maturation process is associated with upregulation of costimulatory molecules and antigen-presenting molecules (22–24). We thus evaluated by flow cytometry the upregulation of essential molecules for DC function in mock-infected and infected cells stimulated with poly-I·C to induce maturation. PPRV-infected mMoDC showed higher expression of PAMP-associated molecules CD14 and CD209 than mock-infected counterparts (Fig. 7A). Expression of adhesion molecules CD11b and CD11c was higher in PPRV-infected cells, although this was not statistically significant. Expression of costimulatory molecule CD86 and antigen-presenting molecules MHC-I and MHC-II was lower in infected cells than in mock-infected counterparts. Costimulatory molecule CD80 expression also tended to be lower in infected cells. Expression of non-classical antigen-presenting molecules CD1 and CD1w2 (CD1b) did not show statistical differences between treatments in mMoDC. Thus, PPRV infection reduces the surface expression on mMoDC of costimulatory and MHC molecules, which are necessary for T cell activation. To determine whether this reduction had an effect on the antigen-presenting capacity of infected mMoDC, we performed mixed lymphocyte reactions (MLR) using these cells as antigen-presenting cells for allogeneic T cells. As shown in Fig. 7B, PPRV-infected mMoDC were unable to stimulate a primary MLR, whereas mock-infected mMoDC could. These data demonstrate that PPRV infection of MoDC resulted in a functional deficit that aborts primary MLR.

The DC phenotype triggered by the infection (reduced upregulation of surface MHC and costimulatory molecules and impaired antigen-presenting capacity)

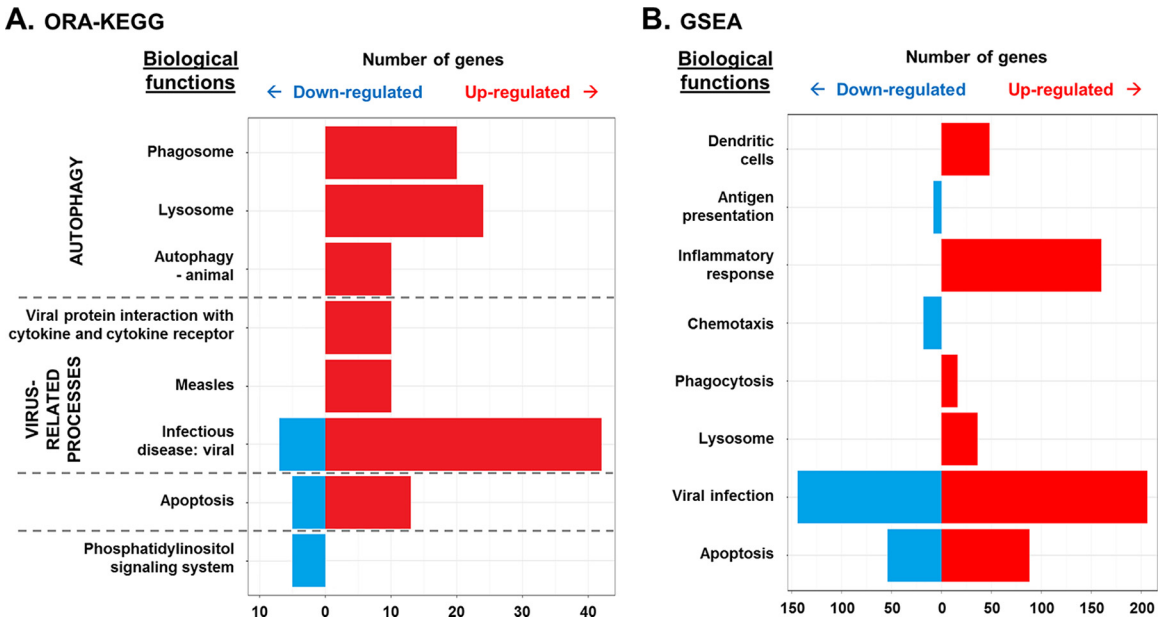

FIG 6 Multiple biological functions are affected by PPRV infection in mMoDC. Number of genes involved in statistically significant upregulated (red) and downregulated (blue) biological functions related to immune processes (dendritic cells, antigen presentation, inflammatory response, chemotaxis, and phagocytosis), autophagy regulation (lysosome, phagosome, and animal autophagy), viral infection (viral infection, infection disease: viral, measles, viral protein interaction with cytokine and cytokine receptor interaction), apoptosis, and second messenger signaling (phosphatidylinositol signaling system) obtained by (A) ORA-KEGG or (B) GSEA analysis in PPRV-infected mMoDC compared to mock-infected mMoDC.

could be due to the virus maintaining the DC at an immature stage. To test this possibility, the antigen uptake capability of PPRV-infected mMoDC was studied. Microsphere phagocytosis assay showed a decrease in the phagocytic capacity in both PPRV- and mock-infected mMoDC compared with iMoDC independently of their infection status, which is indicative of the maturation process (Fig. 7C and D). Importantly, no differences between infected and mock-infected mMoDC were detected, indicating that PPRV-infected mMoDC also reached a maturation stage in which antigen capture is downregulated. A slight decrease in the phagocytic activity of infected iMoDC compared to that of mock-infected cells was observed, although this did not reach significance (Fig. 7D). Thus, PPRV-infected DC do not retain an immature phenotype after poly-I·C treatment, but the infection appears to impair their immunogenic maturation.

PPRV promotes a tolerogenic maturation process in ovine MoDC. Given the impaired immunogenic capacity of PPRV-infected MoDC, we sought out the expression of tolerogenic DC signature genes in our transcriptomic data set. While upregulation of prototypical proinflammatory gene sets appears to a common feature of immunogenic and tolerogenic DC maturation (25), expression of IL-6-associated genes and interferon-stimulated genes (ISG) could be discriminatory between the two maturation processes in mice. Interestingly, few IL-6-associated genes and ISG were upregulated in PPRV-infected mMoDC (Fig. 8A and B). Indeed, we found that STAT2, one of the hallmarks of immunogenic DC maturation in mice (25), was downregulated in infected mMoDC, while several genes involved in the negative regulation of IL-6 were upregulated (e.g., C5AR2, GBA, IL-10, NLRP12, TNFAIP3, and ZC3H12A). Signature genes for tolerogenic DC have been described previously (26–29), and we found that the expression of several of these genes was upregulated in PPRV-infected mMoDC (Fig. 8C). The expression of transcription factors involved in modulating the DC maturation profile was also altered in infected cells compared to that in mock-infected cells (Fig. 8D). These include the downregulation of GATA3, whose expression on DC was shown to promote Th2 responses (30), or the upregulation of NR1D2, a repressor of the ROR

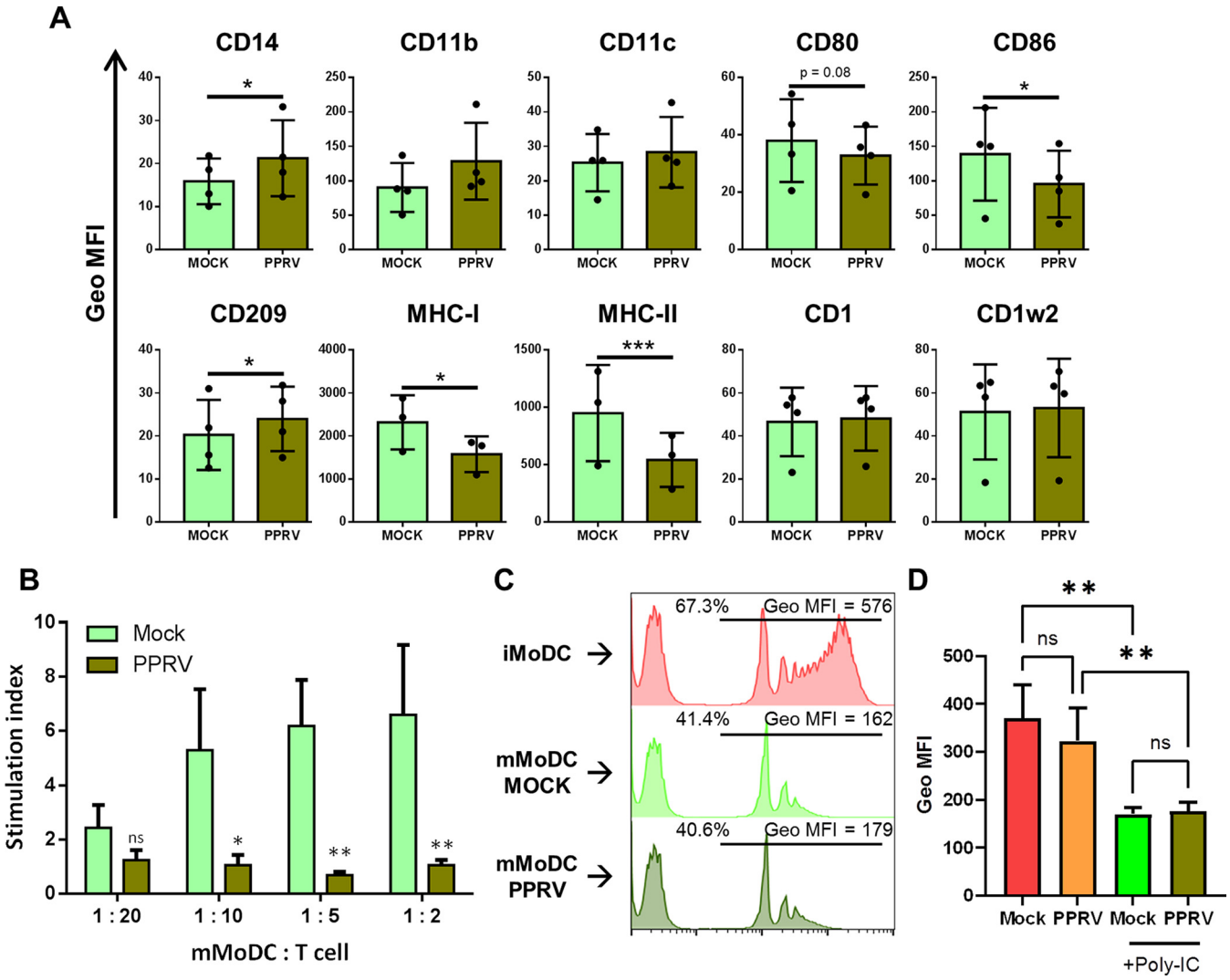

FIG 7 PPRV infection impairs mMoDC function. (A) Geo MFI of cell surface markers (mean ± SD) measured by flow cytometry in mock-infected (bright green) and PPRV-infected (dark green) mMoDC measured in 3 or 4 donor sheep. ns, not significant; *, $P < 0.05$; ***, $P < 0.001$; multiple-ratio paired *t* test with Bonferroni-Dunn correction. (B) Allogeneic mixed lymphocyte reactions (MLR) using mock-infected (bright green) or PPRV-infected (dark green) mMoDC to stimulate T cells at the indicated mMoDC/T cell ratios. T cell proliferation was assessed by [^{3}H]thymidine incorporation in 6-day cocultures. Representative data are presented as mean ± SD of stimulation index (ratio of coculture cpm to T cell-alone cpm). *, $P < 0.05$; **, $P < 0.01$; two-way ANOVA with Tukey's posttest. (C) Representative histograms of microsphere phagocytosis assay assessed by flow cytometry showing the percentage of cells and MFI of beads captured by mock-infected (bright green) or PPRV-infected (dark green) mMoDC compared to iMoDC (red). (D) Geo MFI (mean ± SD; $n = 3$) of mock-infected or PPRV-infected MoDC prior and after Poly-IC treatment in Crimson bead phagocytosis assays. **, $P < 0.01$; one-way ANOVA with Tukey's posttest.

response elements (31) used by the transcription factor ROR-γT, expressed on murine immunogenic mature classical DC2 (cDC2) (32). Furthermore, the downregulation in PPRV-infected mMoDC of the expression of several genes involved in antigen presentation, such as those encoding the MHC-II-like molecule DO (involved in MHC-II molecule peptide loading) (33), or the aminopeptidases ERAP1 and ERAP2 (involved in peptide trimming for MHC-I molecules) (34), indicated that antigen processing may be affected by the infection (Fig. 8E). Overall, the transcription profile of PPRV-infected MoDC indicated that the virus could promote tolerogenic instead of immunogenic DC maturation.

To confirm this hypothesis, we assessed the capacity of PPRV-infected mMoDC to affect T cell responses to the T cell mitogen ConA in an autologous context. Mock- or PPRV-infected mMoDC were cocultured with autologous T cells labeled with CellTrace Violet, and $CD4^+$ and $CD8^+$ T cell proliferation upon ConA stimulation was measured by flow cytometry (Fig. 9). Coculture of T cells with PPRV-infected mMoDC decreased

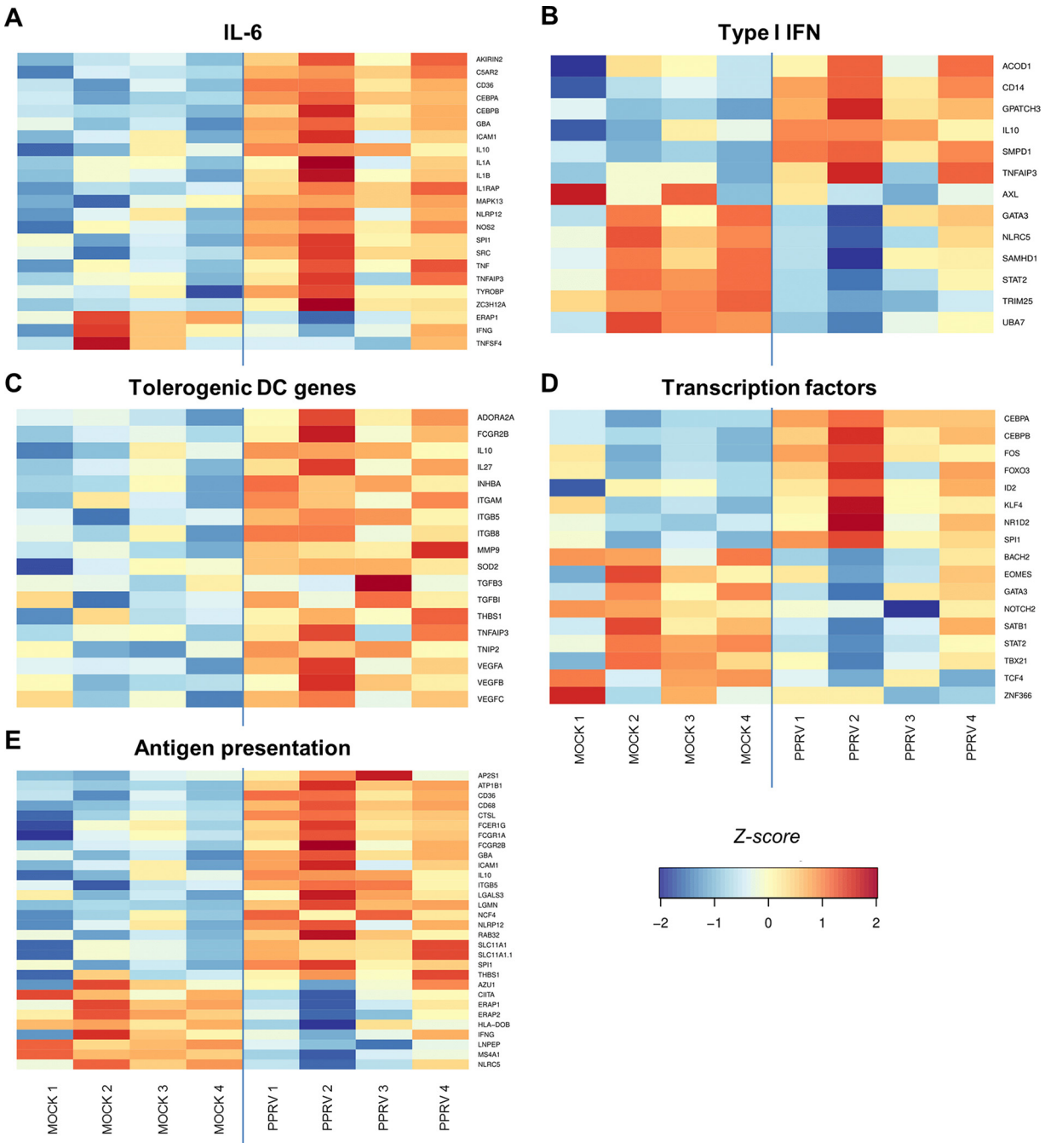

FIG 8 Heatmaps of DEG in PPRV-infected mMoDC related to (A) IL-6, (B) type I IFN, (C) tolerogenic DC genes, (D) transcription factors involved in DC response modulation, and (E) antigen presentation. Gene selection was based on gene onotology (GO) terms for IL-6, type I IFN, and antigen presentation, as well as literature review for tolerogenic DC genes and transcription factors.

the percentage of proliferating $CD4^+$ and $CD8^+$ T cells in response to ConA compared to that in mock-infected counterparts (Fig. 9B and E). A higher CellTrace Violet geometric MFI (Geo MFI) in $CD4^+$ and $CD8^+$ T cell was detected in PPRV-infected cocultures than with mock-infected mMoDC (Fig. 9C and F). As the fluorescence intensity of the dye is halved with each cell division, this higher MFI in PPRV-infected mMoDC cocultures indicated that these infected DC limited the number of T cell divisions in response to ConA. These data suggest that PPRV-infected mMoDC impair $CD4^+$ and $CD8^+$ T cell activation and thus could contribute to host immunosuppression.

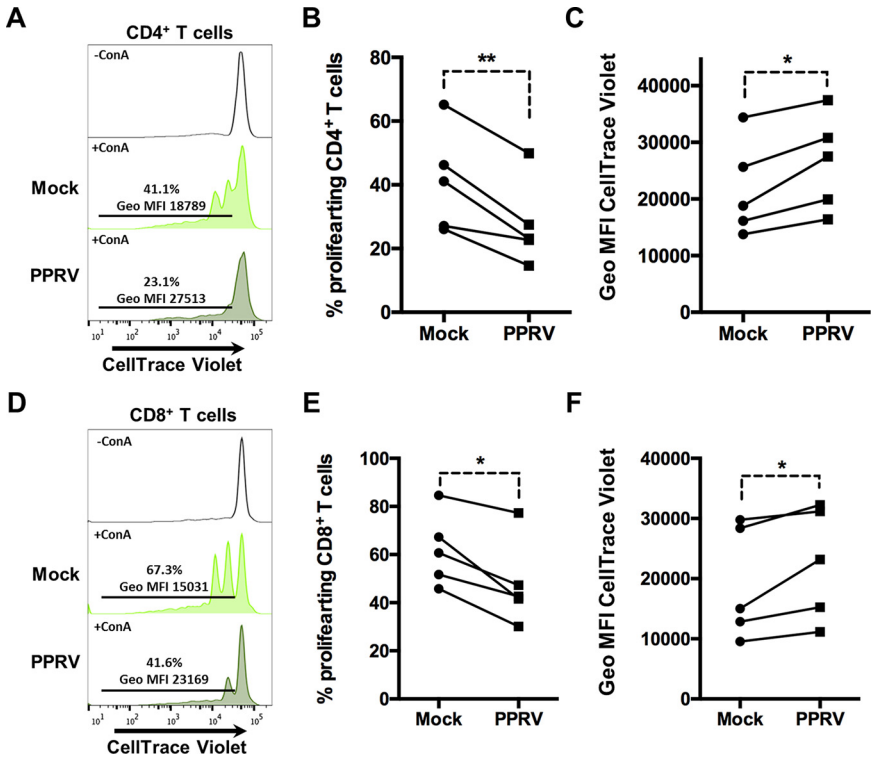

FIG 9 PPRV-infected mMoDC impair CD4$^+$ and CD8$^+$ T cell proliferation. The CellTrace Violet-labeled T cell fraction was cocultured with autologous mock- or PPRV-infected mMoDC and stimulated with the mitogen ConA. Proliferation was assessed by flow cytometry in CD4$^+$ and CD8$^+$ T cells after the relevant antibody surface staining and exclusion of dead cells. (A) Example of CD4$^+$ T cell proliferation in mock- or PPRV-infected mMoDC cocultures. (B and C) Percentage of proliferating cells (B) and Geo MFI (C) in CD4$^+$ T cells in 5 independent experiments. (D) Example of CD8$^+$ T cell proliferation in mock- or PPRV-infected mMoDC cocultures. (E and F) Percentage of proliferating cells (E) and Geo MFI (F) in CD8$^+$ T cells in 5 independent experiments. *, $P < 0.05$; **, $P < 0.01$; paired Student's *t* test.

DISCUSSION

The exact mechanisms that lead to immunosuppression during the acute phase of morbillivirus infection are not fully elucidated. PPRV, like other morbilliviruses, is likely to use multiple immunosuppressive mechanisms to evade immunity and expand its window of replication. PPRV infections are known to produce leukopenia (6, 35), which results in a weakened immune status that is taken advantage of by opportunistic pathogens. We have also observed impaired T cell response to mitogens in infected animals (9, 10). Our data show a significant impact of PPRV infection on DC function, suggesting targeting of DC by PPRV to induce the T cell hyporesponsiveness detected during infection. Several nonexclusive immunosuppressive mechanisms on DC activity have been described for morbillivirus infections, such as promotion of DC apoptosis (36), impaired induction of lymphoproliferation (14, 37, 38), or alteration in DC cytokine response (14, 15).

We have established a reliable *in vitro* differentiation protocol in sheep, a natural host of the disease, for monocyte-derived dendritic cells that produced immature MoDC with high phagocytic ability and mature MoDC with a high capacity to stimulate allogeneic T cells. We found that PPRV could productively infect ovine monocytes *in vitro*. In MV infections, monocytes can also be a natural target of infection that could contribute to virus dissemination and immunosuppression (39). In turn, PPRV infection of monocytes impaired ovine iMoDC differentiation. Differentiating iMoDC infected with PPRV had reduced phagocytic capacity as well as decreased upregulation of antigen-presenting molecules (MHC-II, CD1, and CD1w2), CD11c integrin, and molecules

related to the PAMP recognition (CD14 and CD209). MoDC are a DC population naturally occurring during immune responses in mice and humans that is likely to locally support the role of conventional DC in mounting an immune response (20, 40, 41). Thus, it could be speculated that PPRV potency to infect monocytes, and its subsequent impairment of MoDC differentiation, could be a mechanism to limit the amplitude of the immune response to the infection.

PPRV also productively infects iMoDC and impairs their maturation toward an immunogenic phenotype. Curiously, PPRV production was lower in infected iMoDC than in monocyte precursors. MV has also been shown to be poorly productive in human MoDC (14). Whether this could be due to the existence of mechanisms in the differentiated MoDC that limit viral replication, which would be absent in the monocyte precursors, remains to be determined. We also found that PPRV-infected iMoDC could not be optimally activated by poly (I·C) in contrast to mock-infected cells. This resulted in reduced upregulation of MHC-I and MHC-II molecules as well as costimulatory molecules CD80 and CD86 compared to that in the control. Since our objective was to study the effects of PPRV infection on DC function, we irradiated the mMoDC in our lymphoproliferation experiments to prevent the transmission of infective viral particles from the DC to the T cells. This phenomenon has been documented in MV infections, and it could contribute to impair T cell responses and disseminate the virus through the organism (37, 42). Studies in MV-infected DC have shown the existence of immunosuppressive mechanisms independent of virus transmission in the dialogue between DC and T cells. For instance, MV-infected DC did not mature in response to CD40 ligation (14). Our data show that PPRV-infected mMoDC could not stimulate allogeneic T cell proliferation. We also demonstrated that infected mMoDC limited the proliferation of autologous $CD4^+$ and $CD8^+$ T cells in response to the mitogen ConA. It thus appears that PPRV can effectively suppress T cell responses in the absence of viral replication as no infective virus was detected in the supernatant of the cocultures. These data are in line with studies using MV, in which coculture of infected DC led to unresponsiveness of allogeneic T cells (14, 37, 38) and of autologous T cells stimulated with the mitogen phytohemagglutinin (PHA) (38). Taken together, our data indicate that PPRV infection can modify DC maturation programming to reduce their immunogenic capacity.

Although several reports have described the transcriptomic changes in immune cells during PPRV infections (43–49), none have attempted to characterize the DC response to PPRV infection in a natural host from a transcriptomic perspective. Our analysis of mMoDC showed the activation of multiple signaling pathways in response to infection. On the one hand, genes involved in signaling pathways and biological processes related to viral recognition were significantly upregulated. This is a predictable outcome of infection, since DC possess multiple PRR designed to respond to the presence of PAMP. In murine bone marrow-derived DC, Li et al. also found that PPRV infection triggered the activation of inflammatory responses at the transcriptomic level (48). From a transcriptional perspective, the maturation process of DC through PRR engagement has been associated with the upregulation of prototypical proinflammatory gene sets, and this appears to be irrespective of the functional phenotype (25). Our ORA-KEGG and GSEA of infected mMoDC demonstrated enrichment in the TNF and the NF-κB pathways, both of which are typically linked to proinflammatory responses. We also detected enrichment in TGF-β pathways with both methods in infected mMoDC. TGF-β signaling is canonically considered a regulatory pathway in immunity (50), and it is linked to T regulatory and tolerogenic DC function (51). Expression of ISG has been linked to immunogenic DC maturation in mice (25). GSEA indicated that the genes related to the IFN signaling pathway were mostly downregulated in infected cells. PPRV infection thus appears to impair the differential expression of IFN-related genes in mMoDC in response to poly (I·C) stimulation, which in turn could indicate that immunogenic maturation is impaired. Several PPRV proteins are known to interfere with the IFN response and impair IFN induction and signaling (52–57). These inhibitory mechanisms could therefore also come into play in the host

DC to limit ISG expression and impair the desirable immunogenic maturation required for mounting an appropriate immune response to the virus.

Tolerogenic DC gene signatures have recently been proposed for humans and mice (26–29). We found among PPRV-infected mMoDC DEG that the expression of several tolerogenic signature genes is upregulated. Several of these genes are related to TGF-β activity such as *INHBA*, *THBS1*, *MMP9*, and *ITGB8* (26), which concurs with the pathway enrichment analysis. We also found that the expression of IL-10 was upregulated in infected MoDC. IL-10 is another master regulator of immunity that potently targets T cell activity (58). IL-10 overexpression has also been reported to canine MoDC infected with the morbillivirus CDV (15). In MV infections, as well as other viral infections, IL-10 induction in DC has also been linked to DC immunosuppression (14, 59). It could thus be speculated that IL-10 production by PPRV-infected MoDC could also contribute to the T cell immunosuppressive capacity of these cells.

Several reports have also recently defined some of the transcription factors that govern the differential functional maturation of DC subsets (32, 60, 61). Most of these transcription factors have been identified for murine classical DC (cDC) and plasmacytoid DC (pDC) populations, and the extrapolation of these findings to MoDC from a different species should therefore be done with caution. It should nonetheless be noted that bovine cDC1, cDC2, and pDC populations have been characterized (62), and it can therefore be predicted that similar DC subsets exist in sheep. Interestingly, given the immunosuppressive phenotype of PPRV-infected DC, several key transcription factors involved in DC subset functions are downregulated while others are upregulated. The transcription factors SPI1 and KLF4 are upregulated in infected MoDC. SPI1 is critical for cDC and MoDC development but not for their maturation (60, 63). The overexpression of *SPI1* could be interpreted as an inability of the DC to commit to an immunogenic phenotype. On the other hand, *KLF4* expression in murine cDC2 is associated with Th2 immunity involved in parasite clearance (61), which could indicate that PPRV-infected DC would promote a Th2 bias. ROR-γT expression in cDC2 has been associated with inflammatory responses (32). The upregulation of *NR1D2*, a repressor of ROR response elements (31), indicated that the proinflammatory activity of the ROR-γT transcription factors may be impaired in infected MoDC. The expression of transcription factor ZNF366, also known as *DC-SCRIPT*, associated with cDC1 maturation is downregulated in infected cells. cDC1 are critical for mounting immune responses against intracellular pathogens such as viruses (64). The downregulation of *ZNF366* as well as the lack of ISG induction in PPRV-infected MoDC further confirms that these cells are not optimally programmed to prime an antiviral T cell response. Taken together, these data could indicate that PPRV skews MoDC maturation toward a phenotype that would not effectively combat the viral infection. Further work will be nonetheless required to better characterize the transcription factors that govern the different DC subset programming in sheep and to what extent findings in mice can be extrapolated to ruminants and MoDC.

These transcriptomic findings along with the observation that infected mMoDC cannot stimulate the proliferation of allogeneic T cells and impair T cell responses to mitogen indicate that PPRV likely skews MoDC maturation toward a tolerogenic phenotype. It would be interesting in future experiments to assess whether PPRV acts similarly on the different DC populations that exist *in vivo*, such as cDC subsets or pDC. These studies could help elucidate the paradoxical immune response that PPRV, and more generally morbilliviruses, triggers, in which long-lasting immunity is induced to the virus while severe immunosuppression is taking place.

Transcriptomic analysis of mMoDC also revealed that PPRV modulates the autophagy and apoptosis in infected cells. PPRV has been reported to induce apoptosis in goat peripheral blood mononuclear cells (PBMC) (65), a mechanism that could contribute to the characteristic leukopenia induced by the infection. However, the concomitant upregulation of genes related to autophagy could indicate that the viral infection prevents mMoDC apoptosis. Autophagy is an important mechanism for PPRV replication (66, 67) that inhibited

caspase-dependent apoptosis in PPRV-infected caprine endometrial epithelial cells (68). ORA-KEGG and GSEA concurred in the upregulation of AMPK, mTOR, and PI3K-Akt pathways in infected cells, all of which are central to autophagy regulation. Given AMPK's role as a sensor of cell energetic requirements (69), several viruses are known to modulate AMPK signaling during infection to benefit their energy requirement for replication and promote autophagy (70–72). PI3K signaling is also a route activated by nonsegmented negative-strand RNA viruses, such as paramyxoviruses, to limit apoptosis and increase their intracellular replication window (73). Our data indicate that PPRV can also manipulate the AMPK-mTOR-PI3K axis in DC during infection, probably to promote autophagy and enhance viral replication. It would be interesting in future experiments to assess the balance between apoptosis and autophagy triggered in immune cells targeted by infection, such as DC or lymphocytes.

To the best of our knowledge, the present work is the first report on the effects of PPRV infection on the functionality of ovine $CD14^+$ cells differentiating into iMoDC and on the maturation of MoDC. We provide evidence of the capacity of the morbillivirus PPRV to impair monocyte-derived dendritic cell differentiation and maturation. Transcriptomic analysis indicated that PPRV produced a reprogramming of mMoDC activation that promoted a tolerogenic rather than an immunogenic DC phenotype. These data provide further insight into the mechanisms employed by PPRV to suppress immunity and thereby promote its replication. Understanding the complex network of interactions that take place during morbillivirus infection will surely help improve the treatment of the debilitating diseases that these viral infections produce.

MATERIALS AND METHODS

Cell lines and viruses. Vero cells expressing Dog-SLAM (VDS cells) (provided by S Parida, Pirbright, UK) were cultured in Dulbecco modified Eagle medium (DMEM) with 1% fetal bovine serum (FBS), 2 mM L-Gln, 1% 100× nonessential amino-acids, 1 mM sodium pyruvate, 100 U/mL penicillin–100 μg/mL streptomycin, and 1 μg/mL phleomycin D1 (Zeocin). PPRV Ivory Coast'89 (PPRV ICV'89, lineage I) isolate, kindly provided by CA Batten (Pirbright, UK), was used in all the experiments. PPRV ICV'89 stocks were grown in VDS cells and quantified by plaque assays in VDS cells previously described (9).

Generation of ovine monocyte-derived DC and infection. Blood from healthy donor ewes housed at the Department of Animal Reproduction (INIA, Madrid, Spain) was obtained to isolate peripheral blood mononuclear cells (PBMC) by Ficoll gradient separation technique, as previously described (74). A human CD14 magnetic bead isolation kit (Miltenyi Biotec) was used for positive selection of CD14 cell-enriched fractions (at least 85%) following the manufacturer's protocol. To differentiate $CD14^+$ monocytes into immature monocyte-derived DC (iMoDC), $CD14^+$ cell-enriched fractions were cultured in 6-well plates at 3×10^6 cells/well in 1.5 mL complete RPMI (RPMI with 10% FBS, 2% HEPES, 2 mM L-Gln, 1% 100× nonessential amino-acids, 1 mM sodium pyruvate, 100 U/mL penicillin/100 μg/mL streptomycin, and 50μM 2-mercaptoethanol) supplemented with 20 ng/mL ovine GM-CSF (OvGM-CSF) (Kingfisher Biotech) and 20 ng/mL ovine IL-4 (OvIL-4) (Kingfisher Biotech), and incubated at 37°C, 5% CO_2, and >90% humidity for 72 h. To obtain mature monocyte-derived DC (mMoDC), iMoDC cultures were further supplemented with 20 ng/mL OvGM-CSF and 20 ng/mL OvIL-4 at 48 h, and, to induce maturation, transfected at 72 h with 2.5 μg poly (I·C) (Invivogen)/1×10^6 cells cultures using Lipofectamine 3000 reagent (Thermo Fisher Scientific) following the manufacturer's instructions. mMoDC were ready for use 24 h posttransfection. To assess PPRV effects on iMoDC differentiation, $CD14^+$ monocytes were infected (0 h) at MOI of 1 and subsequently differentiated with OvGM-CSF and OvIL-4 for 72 h. To assess PPRV effects on iMoDC maturation, iMoDC differentiated for 48 h were infected at MOI of 1 and matured the following day (72-h culture) with an overnight poly (I·C) stimulation. mMoDC were harvested 24 h later for analysis (i.e., at 48 h postinfection [hpi]).

Flow cytometry and cell marker antibodies. Cells were stained with primary antibodies diluted in PBS stain buffer (PBS, 2% FBS, 0.03% sodium azide) for 20 min on ice. After that, cells were washed and incubated with secondary antibodies (when required) under the same conditions, followed by 1% paraformaldehyde (PFA) fixation. For intracellular staining, cells were fixed in 4% PFA, permeabilized, and stained in PBS stain buffer supplemented with 0.2% saponin. The following antibodies were used in this study: anti-CD14 (clone TÜK4; Bio-Rad), anti-CD11b (clone MM12A; Kingfisher Biotech), anti-CD11c (clone BAQ153A; Kingfisher Biotech), anti-CD80 (clone IL-A159; Bio-Rad), anti-CD86 (clone IL-A190,; Bio-Rad), anti-CD209 (clone 209MD26A; Kingfisher Biotech), anti-MHC-I (clone 41.17; Bio-Rad), anti-MHC-II (clone 49.1; Bio-Rad), anti-CD1 (clone 20.27; Bio-Rad), anti-CD1w2 (CD1b) (clone CC20; Bio-Rad), and anti-PPRV-N monoclonal antibody (for PPRV detection, intracellular staining; gifted by G Libeau, CIRAD, Montpellier, France). Rat anti-mouse IgM fluorescein isothiocyanate (FITC) (clone II/41; BD Biosciences), polyclonal goat anti-mouse IgG R-phycoerythrin (RPE) (Biolegend), rat anti-mouse IgG1 RPE (clone RMG1-1; Biolegend), and polyclonal goat anti-mouse IgG A647 (Thermo Fisher) were used as secondary antibodies. All appropriate isotype and secondary controls were included. Flow cytometry was also used to study apoptosis dynamics, comparing mock- and PPRV-infected iMoDC at 24, 48, and 72 h, with Annexin V and 7-AAD staining using the Annexin V-phycoerythrin (PE) apoptosis detection kit I (BD Biosciences), and following the

manufacturer's instructions. In some experiments, 7-AAD was used to discriminate live from dead cells. Samples were acquired on a FACSCalibur flow cytometer (BD Biosciences), and data were analyzed with FlowJo v10 software (FlowJo, LLC).

Phagocytosis assays and immunofluorescence confocal microscopy. $CD14^+$ cell, iMoDC, and mMoDC phagocytosis capabilities were quantified by microsphere phagocytosis assays. Crimson fluorescent (625/645) FluoSpheres carboxylate-modified 1.0-μm Microspheres (Thermo Fisher) were added to the cultures at a 20:1 microsphere/cell ratio and incubated for 4 h. Flow cytometry analysis was carried out on $CD14^+$ cell, iMoDC, and mMoDC mock- or PPRV-infected populations to determine the percentage of cells positive for microsphere fluorescence and their geometric mean fluorescence intensity (Geo MFI).

For immunofluorescence microscopy studies, 72-hpi mock- or PPRV-infected iMoDC were stained for the DC surface marker CD11b and goat anti-mouse IgG A488 (A-11029, Life Technologies) as secondary antibody using the standard flow cytometry protocol. Cells were then fixed with a 4% paraformaldehyde solution, for 20 min at room temperature (RT). Nuclei were counterstained using 4',6-diamidino-2-phenylindole(DAPI) (Sigma-Aldrich). Finally, cells were laid on slides and mounted using Prolong gold antifade reagent (Invitrogen). Images were captured with a 63× objective using an LSM 880 confocal microscope (Zeiss). For z-stack imaging, captures were performed at 0.2 μm intervals. Image analysis was performed with the ImageJ software (http://rsbweb.nih.gov/ij/).

Allogeneic MLR. T cells (2×10^5/well) were plated in U-bottom 96-well plates in triplicates and cocultured for 5 days with PPRV- or mock-infected mMoDC at different DC/T cell ratios (1:2, 1:5, 1:10, and 1:20). [^{3}H] thymidine (Hartmann Analytic) was added (50 μCi/mL) in the last 24 h. Finally, cells were transferred onto UniFilter-96 microplates (Perkin-Elmer) with a cell harvester. Incorporated [^{3}H] thymidine was registered on a 1450 MicroBeta Trilux scintillation counter (PerkinElmer). The allogeneic T cell-enriched fraction used in these assays was obtained as described previously (75). Briefly, PBMC were depleted in $CD14^+$ cells with the human CD14 isolation kit (Miltenyi Biotec). The CD14-depleted fraction was then enriched in T cells by nylon wool column separation (75, 76). $CD14^-$ PBMC were incubated in a medium-equilibrated nylon wool column for 45 min at 37°C, 5% CO_2, and >90% humidity, followed by collection of the first 14 mL T cell-enriched eluate (typically >70%). Separation efficiency was checked by flow cytometry. DC were irradiated with 1,500 rads prior to coculture to inactivate virus replication and prevent putative DC culture proliferation. The supernatant of MLR cultures showed no plaque formation in VDS cell plaque assays for PPRV, which confirmed virus inactivation.

Flow cytometry-based proliferation assays. CD14-depleted T cell-enriched fractions prepared as described above (75, 76) and labeled with CellTrace Violet (Thermo Fisher) as described in the manufacturer's protocol were cocultured with irradiated autologous mock- or PPRV-infected mMoDC at a ratio of 5 T cells to 1 mMoDC in U-bottom 96-well plates. Cocultures were left unstimulated as a control or stimulated 4 h later with a 1.25 μg/mL of the T cell mitogen ConA (Sigma-Aldrich). After 96-h coculture, cells were labeled with the Live/Dead fixable near-infrared (IR) dead cell stain kit (Thermo Fisher) as described in the manufacturer's protocol and subsequently labeled with anti-ovine CD4 (clone 44.38; Bio-Rad) and anti-ovine CD8 (clone 38.65; Bio-Rad) antibodies. Appropriate unlabeled, isotype, and fluorescence-minus-one controls were used. Samples were acquired on a FACSCelestaSORP flow cytometer (BD Biosciences), and analysis was performed with FlowJo v.10 software by gating on live $CD4^+$ or $CD8^+$ positive events.

RNA isolation and sequencing. RNA from eight mMoDC cultures (four PPRV infected [48 hpi] and four mock infected) was isolated with a RNeasy minikit plus DNase set (Qiagen). RNA integrity number (RIN) was checked to confirm sample quality, which rendered values higher than 5.8. mRNA was captured through the poly(A) tail. Libraries were constructed with a NEBNext Ultra II RNA library prep kit (New England BioLabs) and sequenced on the NextSeq 500 platform (1×75 pb, 20×106 to 25×106 reads/sample) at the Unidad de Genómica, Parque Científico de Madrid.

Raw data processing. Bioinformatic workflow for RNA-seq data analysis is shown in Fig. S1 in the supplemental material. Quality control checks for raw sequence data from each sample were performed using FastQC v.0.11.9 (Babraham Bioinformatics). No adapter contamination or overrepresented sequences were found. Low-quality reads (mean quality score < 15; read length < 36) were removed using Trimmomatic v.0.39 (77), retaining 97.5% of the reads for all samples.

Identification of differentially expressed genes. Mapping of the quality-filtered reads to the *Ovis aries* reference genome was performed using subread-align (Subread v.2.0.1) (78, 79). Then, Cuffdiff (Cufflinks v.2.2.1) (80) was used to perform gene count summarization and to identify differentially expressed genes (DEG) between the PPRV-infected mMoDC samples and their mock-infected counterparts. False-discovery rate (FDR) correction was used to discard false-positive results. Only those genes with a q value lower than 0.05 were considered DEG.

Similarly, mapping to PPRV-ICV'89 genome (GenBank accession no. EU267273.1) was carried out using subread-align, while gene counting was performed using featureCounts tool from the Subread package, based on the annotation provided by GenBank.

Overrepresentation and enrichment analyses. Over-representation analysis (ORA) was carried out employing the Kyoto Encyclopedia of Genes and Genomes (KEGG) pathways and enrichment analysis was performed employing ClusterProfiler v.3.18.1 (81), using the pathways included in the *O. aries*-specific version of the KEGG database. biomarRt v.2.46.3 (82) was used to perform the conversion from Ensembl identifiers (IDs) to Entrez IDs. FDR correction was applied, and pathways with a q value ≤ 0.05 were considered significantly enriched in DEG. Gene-Set Enrichment Analysis (GSEA) carrying out 1,000 *gene_set* permutations with default settings was performed using GSEA program v4.1.0 (83). Gene sets from the C2 v7.4 (*curated gene sets*) collection from the MSigDB database (84) were used. FDR correction was applied and sets with a q-value ≤ 0.05 were considered significantly altered. Since the majority of

sets described very specific processes, these were grouped within different biological functions and signaling pathways categories to aid in data interpretation (Table S1 and S2).

Statistical analysis. Statistical analysis was performed with GraphPad Prism 6 software. Statistical tests used for data analysis are stated in the figure legends.

Data availability. The transcriptomic data set is deposited in GEO with accession number GSE203515.

SUPPLEMENTAL MATERIAL

Supplemental material is available online only.

SUPPLEMENTAL FILE 1, PDF file, 1 MB.

ACKNOWLEDGMENTS

This work has been funded by grants RTI2018-094616-B-100 from the Spanish Ministry of Science and Innovation and VetBioNet INFRAIA-2016-73014 from EU-H2020.

Conceptualization: J.M.R.; N.S.; Data curation: I.G.-G.; Formal Analysis: D.R.-M.; I.G.-G.; Funding acquisition: V.M.; N.S.; Investigation: D.R.-M.; V.M.; J.M.R.; Methodology: D.R.-M.; I.G.-G.; J.M.R.; V.M.; N.S.; Project administration: V.M.; N.S.; Resources D.R.-M.; V.M.; J.M.R.; N.S.; Software I.G.-G.; Supervision V.M.; J.M.R.; N.S.; Validation D.R.-M.; I.G.-G.; J.M.R.; N.S.; Visualization: D.R.-M.; I.G.-G.; Writing – original draft: D.R.-M.; I.G.-G.; J.M.R.; N.S.; Writing – review & editing: J.M.R.; N.S.

REFERENCES

1. Gargadenec L, Lalanne A. 1942. La peste des petite ruminants. Bull Serv Zoot Epizoot AOF 5:16–21.
2. Banyard AC, Parida S, Batten C, Oura C, Kwiatek O, Libeau G. 2010. Global distribution of peste des petits ruminants virus and prospects for improved diagnosis and control. J Gen Virol 91:2885–2897. https://doi.org/10.1099/vir.0.025841-0.
3. Kumar N, Maherchandani S, Kashyap SK, Singh SV, Sharma S, Chaubey KK, Ly H. 2014. Peste des petits ruminants virus infection of small ruminants: a comprehensive review. Viruses 6:2287–2327. https://doi.org/10.3390/v6062287.
4. FAO/World Organisation for Animal Health. 2015. Global strategy for the control and eradication of PPR. http://wwwfao.org/3/i4460e.pdf.
5. Pfeffermann K, Dörr M, Zirkel F, von Messling V. 2018. Morbillivirus pathogenesis and virus–host interactions. Adv Virus Res, 100:75–98.
6. Pope RA, Parida S, Bailey D, Brownlie J, Barrett T, Banyard AC. 2013. Early events following experimental infection with Peste-Des-Petits ruminants virus suggest immune cell targeting. PLoS One 8:e55830. https://doi.org/10.1371/journal.pone.0055830.
7. Prajapati M, Alfred N, Dou Y, Yin X, Prajapati R, Li Y, Zhang Z. 2019. Host cellular receptors for the peste des petits ruminant virus. Viruses 11:729. https://doi.org/10.3390/v11080729.
8. Tatsuo H, Ono N, Yanagi Y. 2001. Morbilliviruses use signaling lymphocyte activation molecules (CD150) as cellular receptors. J Virol 75:5842–5850. https://doi.org/10.1128/JVI.75.13.5842-5850.2001.
9. Rojas JM, Moreno H, Valcarcel F, Pena L, Sevilla N, Martin V. 2014. Vaccination with recombinant adenoviruses expressing the peste des petits ruminants virus F or H proteins overcomes viral immunosuppression and induces protective immunity against PPRV challenge in sheep. PLoS One 9:e101226. https://doi.org/10.1371/journal.pone.0101226.
10. Rodríguez-Martín D, Rojas JM, Macchi F, Franceschi V, Russo L, Sevilla N, Donofrío G, Martín V. 2021. Immunization with bovine herpesvirus-4-based vector delivering PPRV-H protein protects sheep from PPRV challenge. Front Immunol 12:705539. https://doi.org/10.3389/fimmu.2021.705539.
11. Banchereau J, Steinman RM. 1998. Dendritic cells and the control of immunity. Nature 392:245–252. https://doi.org/10.1038/32588.
12. Adema GJ. 2009. Dendritic cells from bench to bedside and back. Immunol Lett 122:128–130. https://doi.org/10.1016/j.imlet.2008.11.017.
13. Cella M, Salio M, Sakakibara Y, Langen H, Julkunen I, Lanzavecchia A. 1999. Maturation, activation, and protection of dendritic cells induced by double-stranded RNA. J Exp Med 189:821–829. https://doi.org/10.1084/jem.189.5.821.
14. Servet-Delprat C, Vidalain PO, Bausinger H, Manié S, Le Deist F, Azocar O, Hanau D, Fischer A, Rabourdin-Combe C. 2000. Measles virus induces abnormal differentiation of CD40 ligand-activated human dendritic cells. J Immunol 164:1753–1760. https://doi.org/10.4049/jimmunol.164.4.1753.
15. Qeska V, Barthel Y, Herder V, Stein VM, Tipold A, Urhausen C, Günzel-Apel AR, Rohn K, Baumgärtner W, Beineke A. 2014. Canine distemper virus infection leads to an inhibitory phenotype of monocyte-derived dendritic cells in vitro with reduced expression of co-stimulatory molecules and increased interleukin-10 transcription. PLoS One 9:e96121. https://doi.org/10.1371/journal.pone.0096121.
16. Sevilla N, Kunz S, Holz A, Lewicki H, Homann D, Yamada H, Campbell KP, de La Torre JC, Oldstone MB. 2000. Immunosuppression and resultant viral persistence by specific viral targeting of dendritic cells. J Exp Med 192:1249–1260. https://doi.org/10.1084/jem.192.9.1249.
17. Sevilla N, McGavern DB, Teng C, Kunz S, Oldstone MB. 2004. Viral targeting of hematopoietic progenitors and inhibition of DC maturation as a dual strategy for immune subversion. J Clin Invest 113:737–745. https://doi.org/10.1172/JCI20243.
18. Melzi E, Caporale M, Rocchi M, Martin V, Gamino V, di Provvido A, Marruchella G, Entrican G, Sevilla N, Palmarini M. 2016. Follicular dendritic cell disruption as a novel mechanism of virus-induced immunosuppression. Proc Natl Acad Sci U S A 113:E6238–E6247. https://doi.org/10.1073/pnas.1610012113.
19. Tibúrcio R, Nunes S, Nunes I, Rosa Ampuero M, Silva IB, Lima R, Machado Tavares N, Brodskyn C. 2019. Molecular aspects of dendritic cell activation in leishmaniasis: an immunobiological view. Front Immunol 10:227. https://doi.org/10.3389/fimmu.2019.00227.
20. Cheong C, Matos I, Choi JH, Dandamudi DB, Shrestha E, Longhi MP, Jeffrey KL, Anthony RM, Kluger C, Nchinda G, Koh H, Rodriguez A, Idoyaga J, Pack M, Velinzon K, Park CG, Steinman RM. 2010. Microbial stimulation fully differentiates monocytes to DC-SIGN/CD209(+) dendritic cells for immune T cell areas. Cell 143:416–429. https://doi.org/10.1016/j.cell.2010.09.039.
21. Kubicka-Sierszen A, Grzegorczyk JL. 2015. The influence of infectious factors on dendritic cell apoptosis. Arch Med Sci 11:1044–1051.
22. Springer TA. 1990. Adhesion receptors of the immune system. Nature 346:425–434. https://doi.org/10.1038/346425a0.
23. Cella M, Sallusto F, Lanzavecchia A. 1997. Origin, maturation and antigen presenting function of dendritic cells. Curr Opin Immunol 9:10–16. https://doi.org/10.1016/s0952-7915(97)80153-7.
24. Worbs T, Hammerschmidt SI, Forster R. 2017. Dendritic cell migration in health and disease. Nat Rev Immunol 17:30–48. https://doi.org/10.1038/nri.2016.116.
25. Ardouin L, Luche H, Chelbi R, Carpentier S, Shawket A, Montanana Sanchis F, Santa Maria C, Grenot P, Alexandre Y, Grégoire C, Fries A, Vu Manh TP, Tamoutounour S, Crozat K, Tomasello E, Jorquera A, Fossum E, Bogen B, Azukizawa H, Bajenoff M, Henri S, Dalod M, Malissen B. 2016. Broad and largely concordant molecular changes characterize tolerogenic and immunogenic dendritic cell maturation in thymus and periphery. Immunity 45:305–318. https://doi.org/10.1016/j.immuni.2016.07.019.
26. Vendelova E, Ashour D, Blank P, Erhard F, Saliba A-E, Kalinke U, Lutz MB. 2018. Tolerogenic transcriptional signatures of steady-state and pathogen-

induced dendritic cells. Front Immunol 9:333. https://doi.org/10.3389/fimmu.2018.00333.
27. Robertson H, Li J, Kim HJ, Rhodes JW, Harman AN, Patrick E, Rogers NM. 2021. Transcriptomic analysis identifies a tolerogenic dendritic cell signature. Front Immunol 12:733231. https://doi.org/10.3389/fimmu.2021.733231.
28. Nikolic T, Woittiez NJC, van der Slik A, Laban S, Joosten A, Gysemans C, Mathieu C, Zwaginga JJ, Koeleman B, Roep BO. 2017. Differential transcriptome of tolerogenic versus inflammatory dendritic cells points to modulated T1D genetic risk and enriched immune regulation. Genes Immun 18:176–183. https://doi.org/10.1038/gene.2017.18.
29. Castiello L, Sabatino M, Ren J, Terabe M, Khuu H, Wood LV, Berzofsky JA, Stroncek DF. 2017. Expression of CD14, IL10, and tolerogenic signature in dendritic cells inversely correlate with clinical and immunologic response to TARP vaccination in prostate cancer patients. Clin Cancer Res 23:3352–3364. https://doi.org/10.1158/1078-0432.CCR-16-2199.
30. Yashiro T, Kubo M, Ogawa H, Okumura K, Nishiyama C. 2015. PU.1 suppresses Th2 cytokine expression via silencing of GATA3 transcription in dendritic cells. PLoS One 10:e0137699. https://doi.org/10.1371/journal.pone.0137699.
31. Kojetin DJ, Burris TP. 2014. REV-ERB and ROR nuclear receptors as drug targets. Nat Rev Drug Discov 13:197–216. https://doi.org/10.1038/nrd4100.
32. Brown CC, Gudjonson H, Pritykin Y, Deep D, Lavallée V-P, Mendoza A, Fromme R, Mazutis L, Ariyan C, Leslie C, Pe'er D, Rudensky AY. 2019. Transcriptional basis of mouse and human dendritic cell heterogeneity. Cell 179:846–863. https://doi.org/10.1016/j.cell.2019.09.035.
33. Poluektov Y, Kim A, Sadegh-Nasseri S. 2013. HLA-DO and its role in MHC class II antigen presentation. Front Immunol 4:260. https://doi.org/10.3389/fimmu.2013.00260.
34. López de Castro JA. 2018. How ERAP1 and ERAP2 shape the peptidomes of disease-associated MHC-I proteins. Front Immunol 9:2463. https://doi.org/10.3389/fimmu.2018.02463.
35. Rajak KK, Sreenivasa BP, Hosamani M, Singh RP, Singh SK, Singh RK, Bandyopadhyay SK. 2005. Experimental studies on immunosuppressive effects of peste des petits ruminants (PPR) virus in goats. Comp Immunol Microbiol Infect Dis 28:287–296. https://doi.org/10.1016/j.cimid.2005.08.002.
36. Servet-Delprat C, Vidalain PO, Azocar O, Le Deist F, Fischer A, Rabourdin-Combe C. 2000. Consequences of Fas-mediated human dendritic cell apoptosis induced by measles virus. J Virol 74:4387–4393. https://doi.org/10.1128/jvi.74.9.4387-4393.2000.
37. Grosjean I, Caux C, Bella C, Berger I, Wild F, Banchereau J, Kaiserlian D. 1997. Measles virus infects human dendritic cells and blocks their allostimulatory properties for CD4+ T cells. J Exp Med 186:801–812. https://doi.org/10.1084/jem.186.6.801.
38. Schnorr JJ, Xanthakos S, Keikavoussi P, Kämpgen E, ter Meulen V, Schneider-Schaulies S. 1997. Induction of maturation of human blood dendritic cell precursors by measles virus is associated with immunosuppression. Proc Natl Acad Sci U S A 94:5326–5331. https://doi.org/10.1073/pnas.94.10.5326.
39. Esolen LM, Ward BJ, Moench TR, Griffin DE. 1993. Infection of monocytes during measles. J Infect Dis 168:47–52. https://doi.org/10.1093/infdis/168.1.47.
40. Coillard A, Segura E. 2021. Antigen presentation by mouse monocyte-derived cells: re-evaluating the concept of monocyte-derived dendritic cells. Mol Immunol 135:165–169. https://doi.org/10.1016/j.molimm.2021.04.012.
41. Coillard A, Segura E. 2019. In vivo differentiation of human monocytes. Front Immunol 10:1907. https://doi.org/10.3389/fimmu.2019.01907.
42. de Swart RL, Ludlow M, de Witte L, Yanagi Y, van Amerongen G, McQuaid S, Yüksel S, Geijtenbeek TBH, Duprex WP, Osterhaus ADME. 2007. Predominant infection of CD150+ lymphocytes and dendritic cells during measles virus infection of macaques. PLoS Pathog 3:e178. https://doi.org/10.1371/journal.ppat.0030178.
43. Eloiflin RJ, Auray G, Python S, Rodrigues V, Seveno M, Urbach S, El Koulali K, Holzmuller P, Totte P, Libeau G, Bataille A, Summerfield A. 2021. Identification of differential responses of goat PBMCs to PPRV virulence using a multi-omics approach. Front Immunol 12:745315. https://doi.org/10.3389/fimmu.2021.745315.
44. Khanduri A, Sahu AR, Wani SA, Khan RIN, Pandey A, Saxena S, Malla WA, Mondal P, Rajak KK, Muthuchelvan D, Mishra B, Sahoo AP, Singh YP, Singh RK, Gandham RK, Mishra BP. 2018. Dysregulated miRNAome and proteome of PPRV infected goat PBMCs reveal a coordinated immune response. Front Immunol 9:2631. https://doi.org/10.3389/fimmu.2018.02631.
45. Qi X, Wang T, Xue Q, Li Z, Yang B, Wang J. 2018. MicroRNA expression profiling of goat peripheral blood mononuclear cells in response to peste des petits ruminants virus infection. Vet Res 49:62. https://doi.org/10.1186/s13567-018-0565-3.
46. Manjunath S, Mishra BP, Mishra B, Sahoo AP, Tiwari AK, Rajak KK, Muthuchelvan D, Saxena S, Santra L, Sahu AR, Wani SA, Singh RP, Singh YP, Pandey A, Kanchan S, Singh RK, Kumar GR, Janga SC. 2017. Comparative and temporal transcriptome analysis of peste des petits ruminants virus infected goat peripheral blood mononuclear cells. Virus Res 229:28–40. https://doi.org/10.1016/j.virusres.2016.12.014.
47. Wani SA, Sahu AR, Khan RIN, Pandey A, Saxena S, Hosamani N, Malla WA, Chaudhary D, Kanchan S, Sah V, Rajak KK, Muthuchelvan D, Mishra B, Tiwari AK, Sahoo AP, Sajjanar B, Singh YP, Gandham RK, Mishra BP, Singh RK. 2019. Contrasting gene expression profiles of monocytes and lymphocytes from peste-des-petits-ruminants virus infected goats. Front Immunol 10:1463. https://doi.org/10.3389/fimmu.2019.01463.
48. Li L, Wu J, Liu D, Du G, Liu Y, Shang Y, Liu X. 2019. Transcriptional profiles of murine bone marrow-derived dendritic cells in response to peste des petits ruminants virus. Vet Sci 6:95. https://doi.org/10.3390/vetsci6040095.
49. Wani SA, Praharaj MR, Sahu AR, Khan RIN, Saxena S, Rajak KK, Muthuchelvan D, Sahoo A, Mishra B, Singh RK, Mishra BP, Gandham RK. 2021. Systems biology behind immunoprotection of both sheep and goats after Sungri/96 PPRV vaccination. mSystems 6:e00820. https://doi.org/10.1128/mSystems.00820-20.
50. Johnston CJC, Smyth DJ, Dresser DW, Maizels RM. 2016. TGF-β in tolerance, development and regulation of immunity. Cell Immunol 299:14–22. https://doi.org/10.1016/j.cellimm.2015.10.006.
51. Marín E, Cuturi MC, Moreau A. 2018. Tolerogenic dendritic cells in solid organ transplantation: where do we stand? Front Immunol 9:274. https://doi.org/10.3389/fimmu.2018.00274.
52. Rojas JM, Sevilla N, Martin V. 2016. PPRV-induced immunosuppression at the interface of virus-host interaction. Br J Virol 3:140–160. https://doi.org/10.17582/journal.bjv/2016.3.5.140.160.
53. Linjie L, Xiaoling S, Xiaoxia M, Xin C, Ali A, Jialin B. 2021. Peste des petits ruminants virus non-structural C protein inhibits the induction of interferon-β by potentially interacting with MAVS and RIG-I. Virus Genes 57:60–71. https://doi.org/10.1007/s11262-020-01811-y.
54. Li P, Zhu Z, Cao W, Yang F, Ma X, Tian H, Zhang K, Liu X, Zheng H. 2021. Dysregulation of the RIG-I-like receptor pathway signaling by peste des petits ruminants virus phosphoprotein. J Immunol 206:566–579. https://doi.org/10.4049/jimmunol.2000432.
55. Zhu Z, Li P, Yang F, Cao W, Zhang X, Dang W, Ma X, Tian H, Zhang K, Zhang M, Xue Q, Liu X, Zheng H. 2019. Peste des petits ruminants virus nucleocapsid protein inhibits beta interferon production by interacting with IRF3 to block its activation. J Virol 93:e00362-19. https://doi.org/10.1128/JVI.00362-19.
56. Sanz Bernardo B, Goodbourn S, Baron MD. 2017. Control of the induction of type I interferon by peste des petits ruminants virus. PLoS One 12:e0177300. https://doi.org/10.1371/journal.pone.0177300.
57. Ma X, Yang X, Nian X, Zhang Z, Dou Y, Zhang X, Luo X, Su J, Zhu Q, Cai X. 2015. Identification of amino-acid residues in the V protein of peste des petits ruminants essential for interference and suppression of STAT-mediated interferon signaling. Virology 483:54–63. https://doi.org/10.1016/j.virol.2015.03.039.
58. Rojas JM, Avia M, Martín V, Sevilla N. 2017. IL-10: a multifunctional cytokine in viral infections. J Immunol Res 2017:6104054. https://doi.org/10.1155/2017/6104054.
59. Díaz-San Segundo F, Rodríguez-Calvo T, de Avila A, Sevilla N. 2009. Immunosuppression during acute infection with foot-and-mouth disease virus in swine is mediated by IL-10. PLoS One 4:e5659. https://doi.org/10.1371/journal.pone.0005659.
60. Nutt SL, Chopin M. 2020. Transcriptional networks driving dendritic cell differentiation and function. Immunity 52:942–956. https://doi.org/10.1016/j.immuni.2020.05.005.
61. Tussiwand R, Everts B, Grajales-Reyes GE, Kretzer NM, Iwata A, Bagaitkar J, Wu X, Wong R, Anderson DA, Murphy TL, Pearce EJ, Murphy KM. 2015. Klf4 expression in conventional dendritic cells is required for T helper 2 cell responses. Immunity 42:916–928. https://doi.org/10.1016/j.immuni.2015.04.017.
62. Barut GT, Lischer HEL, Bruggmann R, Summerfield A, Talker SC. 2020. Transcriptomic profiling of bovine blood dendritic cells and monocytes following TLR stimulation. Eur J Immunol 50:1691–1711. https://doi.org/10.1002/eji.202048643.
63. Chopin M, Lun AT, Zhan Y, Schreuder J, Coughlan H, D'Amico A, Mielke LA, Almeida FF, Kueh AJ, Dickins RA, Belz GT, Naik SH, Lew AM, Bouillet P, Herold MJ, Smyth GK, Corcoran LM, Nutt SL. 2019. Transcription factor PU.1

promotes conventional dendritic cell identity and function via induction of transcriptional regulator DC-SCRIPT. Immunity 50:77–90. https://doi.org/10.1016/j.immuni.2018.11.010.
64. Durai V, Murphy KM. 2016. Functions of murine dendritic cells. Immunity 45:719–736. https://doi.org/10.1016/j.immuni.2016.10.010.
65. Mondal B, Sreenivasa BP, Dhar P, Singh RP, Bandyopadhyay SK. 2001. Apoptosis induced by peste des petits ruminants virus in goat peripheral blood mononuclear cells. Virus Res 73:113–119. https://doi.org/10.1016/s0168-1702(00)00214-8.
66. Zhang Y, Wu S, Lv J, Feng C, Deng J, Wang C, Yuan X, Zhang T, Lin X. 2013. Peste des petits ruminants virus exploits cellular autophagy machinery for replication. Virology 437:28–38. https://doi.org/10.1016/j.virol.2012.12.011.
67. Wan Y, Chen Y, Wang T, Zhao B, Zeng W, Zhang L, Zhang Y, Cao S, Wang J, Xue Q, Qi X. 2022. PPRV-induced autophagy facilitates infectious virus transmission by the exosomal pathway. J Virol 96:e00244-22. https://doi.org/10.1128/jvi.00244-22.
68. Yang B, Xue Q, Qi X, Wang X, Jia P, Chen S, Wang T, Xue T, Wang J. 2018. Autophagy enhances the replication of peste des petits ruminants virus and inhibits caspase-dependent apoptosis in vitro. Virulence 9:1176–1194. https://doi.org/10.1080/21505594.2018.1496776.
69. Oakhill JS, Steel R, Chen ZP, Scott JW, Ling N, Tam S, Kemp BE. 2011. AMPK is a direct adenylate charge-regulated protein kinase. Science 332:1433–1435. https://doi.org/10.1126/science.1200094.
70. Bhutta MS, Gallo ES, Borenstein R. 2021. Multifaceted role of AMPK in viral infections. Cells 10:1118. https://doi.org/10.3390/cells10051118.
71. Li M, Li J, Zeng R, Yang J, Liu J, Zhang Z, Song X, Yao Z, Ma C, Li W, Wang K, Wei L. 2018. Respiratory syncytial virus replication is promoted by autophagy-mediated inhibition of apoptosis. J Virol 92:e02193-17. https://doi.org/10.1128/JVI.02193-17.
72. Lv S, Xu QY, Sun EC, Zhang JK, Wu DL. 2016. Dissection and integration of the autophagy signaling network initiated by bluetongue virus infection: crucial candidates ERK1/2, Akt and AMPK. Sci Rep 6:23130. https://doi.org/10.1038/srep23130.
73. Sun M, Fuentes SM, Timani K, Sun D, Murphy C, Lin Y, August A, Teng MN, He B. 2008. Akt plays a critical role in replication of nonsegmented negative-stranded RNA viruses. J Virol 82:105–114. https://doi.org/10.1128/JVI.01520-07.
74. Rojas JM, Peña L, Martín V, Sevilla N. 2014. Ovine and murine T cell epitopes from the non-structural protein 1 (NS1) of bluetongue virus serotype 8 (BTV-8) are shared among viral serotypes. Vet Res 45:30. https://doi.org/10.1186/1297-9716-45-30.
75. Rojas JM, Rodriguez-Martin D, Avia M, Martin V, Sevilla N. 2018. Peste des petits ruminants virus fusion and hemagglutinin proteins trigger antibody-dependent cell-mediated cytotoxicity in infected cells. Front Immunol 9:3172. https://doi.org/10.3389/fimmu.2018.03172.
76. Hathcock KS. 1999. T cell enrichment by nonadherence to nylon. Curr Protoc in Immunol 30:3.2.1–3.2.4. https://doi.org/10.1002/0471142735.im0302s30.
77. Bolger AM, Lohse M, Usadel B. 2014. Trimmomatic: a flexible trimmer for Illumina sequence data. Bioinformatics 30:2114–2120. https://doi.org/10.1093/bioinformatics/btu170.
78. Liao Y, Smyth GK, Shi W. 2013. The Subread aligner: fast, accurate and scalable read mapping by seed-and-vote. Nucleic Acids Res 41:e108. https://doi.org/10.1093/nar/gkt214.
79. Liao Y, Smyth GK, Shi W. 2014. featureCounts: an efficient general purpose program for assigning sequence reads to genomic features. Bioinformatics 30:923–930. https://doi.org/10.1093/bioinformatics/btt656.
80. Trapnell C, Williams BA, Pertea G, Mortazavi A, Kwan G, van Baren MJ, Salzberg SL, Wold BJ, Pachter L. 2010. Transcript assembly and quantification by RNA-Seq reveals unannotated transcripts and isoform switching during cell differentiation. Nat Biotechnol 28:511–515. https://doi.org/10.1038/nbt.1621.
81. Yu G, Wang LG, Han Y, He QY. 2012. clusterProfiler: an R package for comparing biological themes among gene clusters. OMICS 16:284–287. https://doi.org/10.1089/omi.2011.0118.
82. Durinck S, Moreau Y, Kasprzyk A, Davis S, De Moor B, Brazma A, Huber W. 2005. BioMart and Bioconductor: a powerful link between biological databases and microarray data analysis. Bioinformatics 21:3439–3440. https://doi.org/10.1093/bioinformatics/bti525.
83. Subramanian A, Tamayo P, Mootha VK, Mukherjee S, Ebert BL, Gillette MA, Paulovich A, Pomeroy SL, Golub TR, Lander ES, Mesirov JP. 2005. Gene set enrichment analysis: a knowledge-based approach for interpreting genome-wide expression profiles. Proc Natl Acad Sci U S A 102:15545–15550. https://doi.org/10.1073/pnas.0506580102.
84. Liberzon A, Subramanian A, Pinchback R, Thorvaldsdóttir H, Tamayo P, Mesirov JP. 2011. Molecular signatures database (MSigDB) 3.0. Bioinformatics 27:1739–1740. https://doi.org/10.1093/bioinformatics/btr260.